

## Theory of tunneling spectroscopy for semiconductors

Fredy R. Zypman

*University of Puerto Rico, Department of Physics and Electronics, Humacao, Puerto Rico 00791*

Luis F. Fonseca

*University of Puerto Rico, Department of Physics, Rio Piedras, Puerto Rico 00931*

Yehuda Goldstein

*The Racah Institute of Physics, The Hebrew University, Jerusalem 91904, Israel*

(Received 3 May 1993; revised manuscript received 17 September 1993)

It is generally accepted that scanning tunneling microscopy and scanning tunneling spectroscopy (STS) get their information from the sample local density of states. At present, however, there is little theoretical ground on which to explore this assumption. We contribute here with a theory of STS for semiconductors, treated within the tight-binding approach. In the context of this theory, we demonstrate that the current-voltage ( $I$ - $V$ ), and the conductance-voltage ( $\sigma$ - $V$ ) curves are related to the density of states. In particular, the current is a sum over tip states of semiconductor local density of states modulated by tip-dependent coefficients. This result is consistent with those found in previous works. The  $\sigma$ - $V$  curve has nondifferentiable points which are a direct manifestation of the Van Hove singularities in the global density of states of the semiconductor.

### I. INTRODUCTION

Scanning tunneling spectroscopy (STS) is a technique used to extract energy spectral information at a particular place on a sample surface from its current-voltage ( $I$ - $V$ ) curve. This has been experimentally achieved on semiconductors,<sup>1-3</sup> superconductors,<sup>4</sup> and metals.<sup>5</sup> Essentially, in STS one locates a tip at a given  $x_0$ - $y_0$  position on top of a surface. Then the tunneling current between tip and sample is measured as the tip-sample voltage is varied. This curve has, in general, to be deconvoluted in order to obtain the desired energy information. The deconvolution itself depends on the system under study and the model used to describe that system.

The way in which the local density of states (LDOS) appears in the  $I$ - $V$  curves has been the subject of extensive theoretical study.<sup>6-14</sup> Most theoretical calculations have obtained results for imaging at low bias voltage, such as the widely used theory of Tersoff and Hamann.<sup>6</sup> Some workers<sup>15-17</sup> have extended these results to finite voltages. We have developed a theory that applies specifically to semiconductors, since they need a special treatment, different from the one for metals.<sup>18-20</sup> Macroscopically, we model the semiconductor as a cube with a free surface. Microscopically we assume that the semiconductor has a simple cubic unit cell. Its band structure is obtained from the tight-binding (TB) approach. The STM tip is assumed to be formed by a single atom (adatom) adsorbed on a surface. The energy structure of this system is also obtained within the TB framework. By choosing appropriate TB parameters, we can account for a metallic tip. We found that for certain choices of TB parameters there exists the possibility of tip states localized around the adsorbed atom. The current between tip and sample is then calculated using

Bardeen's<sup>21,22</sup> tunneling theory. When many tip states (band states, localized states, or a combination of both) contribute to the current, the current is a convolution of the sample LDOS and the tip electron probability function. In the range of voltages for which only a discrete tip state is involved in the tunneling, the current itself is directly proportional to the sample LDOS. We also studied the  $\sigma$ - $V$  curve and found that it followed the sample DOS in some voltage regions.

The situation just described does not take into consideration the tunneling barrier height. For that reason, we also consider the effect that the electric field existing in the tip-sample gap has on the shape of the adatom wave function. Essentially, for positive bias voltage, the wave function will distort so that the electron has a greater probability of being in the gap than towards the tip bulk. This distortion has the effect of increasing the current, but overall the results described above also apply in this case.

### II. THEORY

Before calculating the current in the manner of Bardeen, we need to specify the electronic structure of both the semiconducting sample under study and the metallic tip. Consider the sample to be a semiconductor with simple cubic structure with  $N$  Wigner-Seitz cells on a side. Its energy states are considered in the near-neighbor tight-binding approach<sup>23</sup> with an  $s$ -type basis function (cubium model<sup>24</sup>). This type of approach has been extensively used in the past to study chemisorption on surfaces<sup>24-26</sup> and DOS of surface states.<sup>27</sup> In this context, the wave functions read

$$\psi_{\theta} = \sum_{\mathbf{m}} C_{\theta, \mathbf{m}} \Phi_{\mathbf{m}}, \quad (1)$$

where  $\theta_i$  are the labels for the states,  $\psi_\theta$  are the Hamiltonian eigenstates to be found,  $\Phi_m$  are  $s$ -type atomic orbitals, and  $C_{\theta,m}$  are the expansion coefficients. The vector index  $(m_1, m_2, m_3)$  identifies the atomic sites, and can take  $N^3$  different values.

The corresponding energies are

$$E = \alpha + 2\beta(\cos\theta_1 + \cos\theta_2 + \cos\theta_3), \quad (2)$$

where  $\alpha$  is the Coulomb integral and  $\beta$  the resonance integral.<sup>23</sup>

The coefficients are given by

$$C_\theta(\mathbf{m}) = e^{i(m_1\theta_1 + m_2\theta_2 + m_3\theta_3)}, \quad (3)$$

where  $\theta_1 = 2k_1\pi/N$  etc., in bulk,  $k_1$  being an integer.

The presence of a surface perpendicular to the  $z$  axis modifies the values that  $\theta_3$  can take. Furthermore, if  $\alpha$  and  $\beta$  are the Coulomb and resonance integrals of bulk and  $\alpha'$  is the Coulomb integral of the atoms on the surface, then the parameter  $z \equiv (\alpha - \alpha')/\beta$  controls the behavior of the sample states. In this case, the tight-binding coefficients are given by<sup>28</sup>

$$C_\theta(\mathbf{m}) = e^{i(m_1\theta_1 + m_2\theta_2)} \sin[(N - m_3)\theta_3], \quad (4)$$

where  $\theta_3$  is now one of the  $N$  roots of the equation

$$z + \cos\theta_3 + \sin\theta_3 \cotan(N\theta_3) = 0. \quad (5)$$

For each root, there are  $N^2$  states since  $\theta_1$  and  $\theta_2$  can take  $N$  different values each. The scanning tip is taken as being an atom (adatom) adsorbed onto a surface. The electronic structure of this system is obtained also in the tight-binding context. The qualitative behavior of the electron states has been studied elsewhere.<sup>28</sup> We worked out the problem numerically in order to obtain quantitative results. The main features are described next. Depending on the relationship between the various Coulomb and resonance integrals, the system may have two, one, or no localized states around the adatom position. The energy of these states may lie above or below the surface and bulk bands. The existence of these states changes the qualitative behavior of the STM in the spectroscopic mode, as will be seen below.

Now that we have described the two systems between which the tunneling occurs, we can use Bardeen's approach to calculate the current. Bardeen defined a right and a left system and found that the transition probability for an electron to tunnel between them is<sup>21</sup>

$$M_{RL} = \frac{i\hbar^2}{2m} \int_S \left[ \psi_R \frac{\partial \psi_L}{\partial \xi} - \psi_L \frac{\partial \psi_R}{\partial \xi} \right] dS, \quad (6)$$

where  $\psi_R$  and  $\psi_L$  are the right and left eigenfunctions of the corresponding Hamiltonians,  $S$  is any surface that completely separates the right from the left region,  $m$  is the mass of the electron, and  $\xi$  is a coordinate normal to  $S$ . In the tight-binding approach, both wave functions are a sum of terms at the atomic sites. The total  $M_{RL}$ , better called  $M_{TS}$  for tip-sample system, will then be the sum of the individual  $M_{12}$  of each tip-sample pair of atoms—called 1 and 2. Let us begin by calculating  $M_{12}$ .

The adatom, labeled 1, is located at the origin of our coordinates system as shown in Fig. 1. A generic atom from the sample, labeled 2, is located a distance  $s_m$  away, where  $(m_1, m_2, m_3)$  is the label for that sample site. We take the corresponding wave functions to be

$$\Phi_1(\mathbf{r}) = \frac{1}{\sqrt{\pi a_t^3}} e^{-r/a_t}, \quad (7)$$

$$\Phi_2(\mathbf{r}) = \frac{1}{\sqrt{\pi a_s^3}} e^{-r'/a_s}, \quad (8)$$

$$r' \equiv \sqrt{r^2 + s_m^2 - 2rs_m \cos\gamma}, \quad (9)$$

where  $a_t$  and  $a_s$  are the decay lengths of the tip and sample wave-function basis, respectively, and, at the surfaces, for the following numerical results, they will be taken to be 0.4 and 0.35 Å, to represent tungsten and silicon wave-function decays, respectively<sup>29,30</sup> (since we use spherical wave functions, this can be considered as a fit to the real wave functions and therefore has limitations).

The corresponding transition probability becomes

$$M_{TS} = \frac{iB^2\hbar^2}{m(a_s a_T)^{3/2}} \int_0^\pi d\gamma e^{-B/a_T - r'/a_s} \times \left[ \frac{1}{a_T} - \frac{1}{a_s} \frac{B - s_m \cos\gamma}{r'} \right] \sin\gamma, \quad (10)$$

where the surface  $S$  was considered to be a sphere of radius  $B$  around the adatom.

This integral is readily evaluated in closed form. Under our assumptions, tip and sample are clearly separated

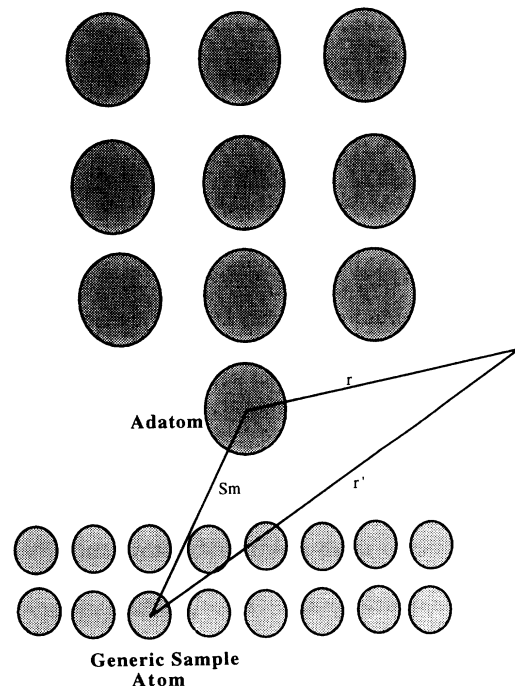


FIG. 1. Sagittal cross section of the atomic arrangement for the tight-binding and  $M_{TS}$  calculations.

objects. This can be accomplished if, for example, the distance  $d$  between tip and sample is large compared with  $a_t$  and  $a_s$ . In that case, the transition matrix element takes the form

$$M_{12} = A e^{-s_m/a_s}, \quad (11)$$

where  $A$  is a constant given by  $ih^2B(1+a_s/a_T)\exp(B/a_s - B/a_T)/[m(a_T a_s)^{3/2}]$ .

As we mentioned before, to calculate  $M_{TS}$  we have to sum the  $M_{12}$ 's over the surface sites. The positions of the atoms on the sample can be parametrized as  $(m_1 a + x_0, m_2 a + y_0, -m_3 a)$  where  $a$  is the lattice parameter. The coordinates  $(x_0, y_0)$  correspond to the place on the surface above which the tip is placed. The wave function of the tip will be truncated from the full tight-binding expansion as

$$\psi_T = C_{\text{adatom}} \psi_{\text{atomic}}(\mathbf{r}). \quad (12)$$

This means that we are considering for the calculation of the current only the tip adatom and the sample atoms. This is a reasonable assumption since  $M_{12}$  decays very fast with the distance between atom 1 and atom 2. One can reasonably ask why the other electrons from the tip surface do not contribute appreciably to the current since there are so many of them. It has been argued<sup>31</sup> that the effective tip surface has about  $20 \times 20 = 400$  atoms. Each one of those atoms are about  $10 \text{ \AA}$  from the sample surface. The adatom instead is about  $2 \text{ \AA}$  away. If the rate of decay of the current with distance is assumed to be about  $63\%/ \text{ \AA}$  (Ref. 32), then the current of all the tip atoms would be  $13\%$  of the current via the single adatom. This is a worst-case scenario. If a discrete state is solely responsible for the tunneling current, its coefficient will account for a very large percentage of the total electron probability.

The total current from tip to sample is then

$$I = \frac{2\pi e A^2}{\hbar} \int \int d\mu_{\text{sample}} d\nu_{\text{tip}} [\theta(E_F^{\text{tip}} - E_{\nu_{\text{tip}}}) - \theta(E_F^{\text{sample}} - E_{\mu_{\text{sample}}})] \times \delta(E_{\mu_{\text{sample}}} - E_{\nu_{\text{tip}}} - V) C_{\nu_{\text{tip}}}^2 \left| \sum_{\mathbf{m}} C_{\mu_{\text{sample}}}(\mathbf{m}) e^{-s_m/a_s} \right|^2, \quad (13)$$

where  $V$  is the voltage applied to the tip. The sample is assumed to be grounded. The parameters  $\mu$  and  $\nu$  are the quantum numbers necessary to completely describe the system, and  $C_\mu$  and  $C_\nu$  the TB coefficients for sample and tip, respectively.

We solved the system numerically for finite  $N$  (it was done for 3, 5, 7, 9, and 11 until the value of the current

converged) so the integral in  $\nu$  will be written as a sum. The continuum sample energy spectrum is exactly known, therefore the integral in sample states will remain, and we make the change of variables from  $\mu$  to  $E_\mu$ , and isoenergy surface parameters.

After integration in  $E_\mu$ ,

$$I = \frac{2\pi e A^2}{\hbar} \sum_{k_{\text{Tip}}=1}^{N^3+1} C^2 k_{\text{Tip}} \int_S \frac{dS_\theta}{|\nabla_\theta E_S|} [\theta(E_F^{\text{Tip}} - E_{k_{\text{Tip}}}) - \theta(E_F^{\text{Sample}} - E_{k_{\text{Tip}}} - V)] \left| \sum_{\mathbf{m}} C_\theta(\mathbf{m}) e^{-s_m/a_s} \right|^2, \quad (14)$$

where  $S$  is the isoenergy surface in  $\theta$  space at  $E_s = E_k^T + V - \alpha_s$ .

Equation (14) will serve as the starting point to obtain  $I-V$  and  $\sigma-V$  curves. Therefore, for consistency, we ask how does this result fit with those obtained in the past by others. One sees that Eq. (14) is at once recognized as a sum of sample LDOS at the energy  $E_s = E_k^{\text{Tip}} + V - \alpha_s$  weighted by the tip wave-function probability at the adatom center,

$$I = \frac{8\pi^2 e A^2}{\hbar} \sum_{k=1}^{N^3+1} C_k^2 [\theta(E_F - E_k^{\text{Tip}}) - \theta(E_F - E_k^{\text{Tip}} - V)] \rho(E_k^{\text{Tip}} + V - \alpha_s), \quad (15)$$

where  $\rho$  is the sample LDOS. This is indeed in agreement with work done on metals,<sup>3,33</sup> and in general at low voltage,<sup>6</sup> and with the closely related work of Ferrer, Martin-Rodero, and Flores,<sup>34</sup> and Sacks and Nogera.<sup>35</sup>

As we mentioned earlier, the model previously described provides for the existence of tip states that have energies outside the continuum band. For a range of voltages, those states will contribute alone to the total current and therefore will provide a direct measurement of the LDOS of the semiconductor within the conduction band. Whether an appropriate tip can be chosen and made, so as to actually realize those discrete states, is an

open issue. However, it is not unreasonable to expect discrete levels for the case in which the electron could be somewhat confined around the adatom. These discrete states may have a high degree of localization, but are not completely localized around the adatom, and its wave function extends into the bulk. This an electron in that state has a nonzero probability of being in bulk, and its "tail" provides for the existence of a nonzero current.

In Fig. 2, the  $I-V$  curve for the case in which a discrete tip state exists below the tip continuum band is shown. The zero-voltage energies of tip and sample corresponding to that plot are shown in Fig. 3. This corresponds to

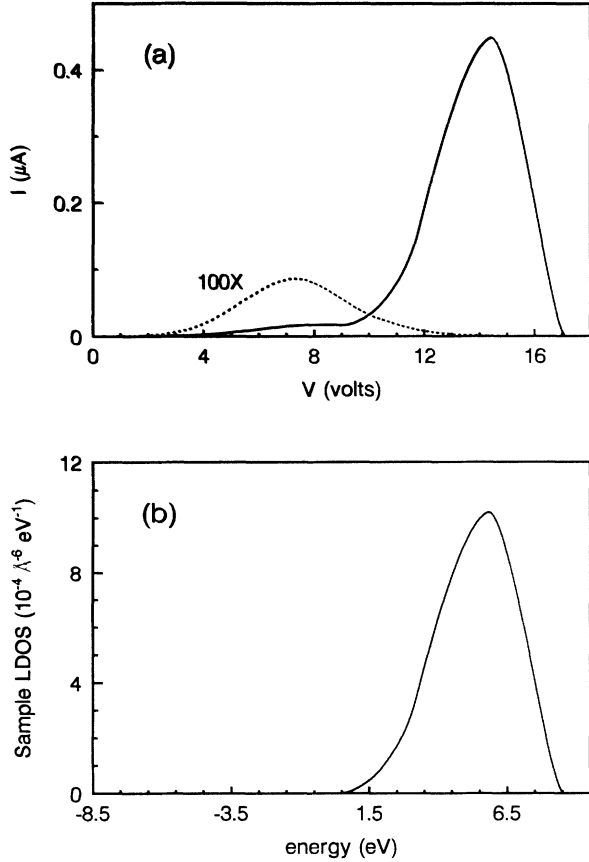


FIG. 2. (a) Plot of current vs voltage for the continuum (dashed line) and discrete (solid line) cases. (b) Sample LDOS. The scales in (a) and (b) have been chosen appropriately so that they can be easily compared.

a sample that has a band gap corresponding to that of silicon.

As the voltage increases from zero, the current remains zero until the tip Fermi level is raised to the bottom of the sample conduction band. This happens when  $E_F + V = E_s^{\text{bottom}}$ . At this point the current starts to increase monotonically up to the moment in which the top of the tip continuum band occupied levels with the top of the sample conduction band. Now the current decreases because fewer and fewer tip states are available for tunneling. After all the states from the tip continuum have gone out of the tunneling range, the discrete state is the only one responsible for the current. Moreover, since the

$$I = \frac{2\pi e A^2}{\hbar} \frac{1}{2\beta_s} \sum_{k=1}^{N^3+1} \int \frac{d\theta_1 d\theta_2}{\sin\theta_3} [\Theta(E_F - E_k^{\text{Tip}}) - \Theta(E_F - E_k^{\text{Tip}} - V)] \times C_k^2 \left| \sum_{m_1 m_2} e^{i(m_1\theta_1 + m_2\theta_2)} \sin(N\theta_3) e^{-[\sqrt{d^2 + (am_1 + x_0)^2 + (am_2 + y_0)^2}]/a_s} \right|^2. \quad (16)$$

The integral of the previous expression is done in the domain  $-\pi < \theta_1 < \pi$ ,  $-\pi < \theta_2 < \pi$  for which

$$\left| \frac{E_k^{\text{Tip}} + V - \alpha_s}{2\beta_s} - \cos\theta_1 - \cos\theta_2 \right| \leq 1. \quad (17)$$

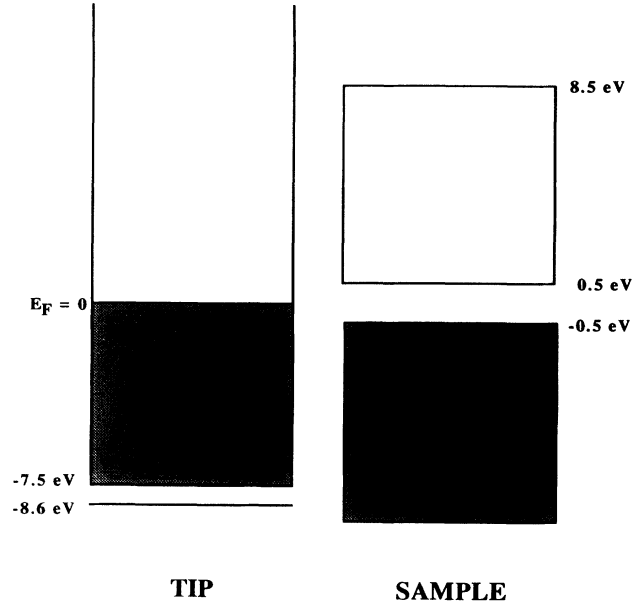


FIG. 3. Energy-level diagrams for the tip and the sample for zero applied voltage for the discrete case. The voltage convention is such that as the bias voltage increases, the tip energy levels more upwards with respect to the sample energy levels. The dark regions represent occupied states. The horizontal line at the bottom of the tip diagram corresponds to the discrete level. The continuum case energy diagram is obtained from this one by just removing the discrete state.

discrete state contributes to the tunneling with the largest TB coefficient, its existence makes the  $I$ - $V$  curve a mapping of the sample LDOS as can be seen by comparing the solid line of Fig. 2(a) with 2(b).

In Fig. 2 we also show the  $I$ - $V$  curve for the continuum case. We see that the current for this last case is about three orders of magnitude smaller than the discrete case current. This is due to the fact that the contribution of the adatom atomic wave function in the sample-tip space gap is much larger in the discrete case, when there exists some localization.

Another issue we wish to address is the relationship between the  $dI/dV$  vs  $V$  curve, and density of states. This is important since many authors have argued that this plot, and not  $I$ - $V$ , is proportional to the LDOS.<sup>36</sup>

Using Eqs. (1) and (2), and transforming the last expression into an integral in Cartesian coordinates in  $\theta$  space,

The sum over sample sites has been reduced to a sum over the sample surface sites. This change shall not affect the physics since the tunneling is due mainly to sample atoms near the tip, and the  $\theta_3$  component of the TB sample coefficient, which, in general, is  $\sin[(N - m_3)\theta_3]$ ,

reduces to a simple form due to the fact that  $m_3=0$ .

Notice in the expression for the current that we have written explicitly the distance between the tip atom and a generic atom. There,  $x_0$  and  $y_0$  are the in-plane coordinates of the tip atom and thus the spectra vary with the lateral position of the tip. In what follows, we show results for the tip positioned above a surface atom.

In order to obtain an explicit dependence of the current on the voltage, we use Eq. (2) to get

$$\sin\theta_3 = \left[ 1 - \left( \frac{E_k^{\text{Tip}} + V - \alpha_s}{2\beta_s} - \cos\theta_1 - \cos\theta_2 \right)^2 \right]^{1/2} \quad (18)$$

and from Eqs. (2) and (5) we can write explicitly  $\sin(N\theta_3)$ ,

$$\sin(N\theta_3) = \left\{ 1 - \left[ \frac{E_k^{\text{Tip}} + V - \alpha_s}{2\beta_s} - \cos\theta_1 - \cos\theta_2 \right]^2 / \left[ 1 + z^2 + 2z \left[ \frac{E_k^{\text{Tip}} + V - \alpha_s}{2\beta_s} - \cos\theta_1 - \cos\theta_2 \right] \right] \right\}^{1/2}. \quad (19)$$

The derivative of  $I$  with respect to  $V$  can be expressed in terms of two different contributions,

$$\frac{dI}{dV} = \sigma_1(V) + \sigma_2(V), \quad (20)$$

where  $\sigma_1$  comes from the derivative of the integrand term with respect to voltage, keeping everything else constant, and  $\sigma_2$  from the derivative of the electron statistical distribution term, keeping the other terms fixed. There could have been an extra contribution to  $dI/dV$  coming from the derivative of the limits of integration with respect to voltage, but it turns out to be zero.  $\sigma_2$  is the usual  $dI/dV$  term, in which the current increases with voltage due to the states at  $E_F - V$  that begin contributing to the tunneling.  $\sigma_1$  depends on the voltage dependence of the tunneling probability—usually unknown.<sup>10</sup> In our model we do know this function explicitly and were able to evaluate the corresponding derivative. The first term has the form

$$\begin{aligned} \sigma_1 = & -\frac{2\pi e^2 A^2}{\hbar} \frac{1}{(2\beta_s)^2} \\ & \times \sum_k c_k^2 \int d\theta_1 d\theta_2 [\Theta(E_F - E_k^{\text{Tip}}) - \Theta(E_F - E_k^{\text{Tip}} - V)] \\ & \times \left[ \frac{\cotan\theta_3}{1 + z^2 + 2z \cos\theta_3} + \frac{2z \sin\theta_3}{(1 + z^2 + 2z \cos\theta_3)^2} \right] \left| \sum_{m_1, m_2} e^{i(m_1\theta_1 + m_2\theta_2)} e^{-(\sqrt{d^2 + \rho_m^2})/a_s} \right|^2. \end{aligned} \quad (21)$$

The function  $\sigma_1(V)$  is shown in Fig. 4. We see that this function presents points at which the slope is discontinuous. These discontinuities come from the Van Hove singularities of the sample. It can be seen from that figure that both curves resemble the sample DOS (see Fig.

5) for voltages between  $V_a$  and  $V_b$ . We will now analyze to what extent this resemblance can be taken as a real relationship between  $\sigma_1$  and DOS. Let us first consider the discrete case. For voltages close to  $V_a$  the integration in

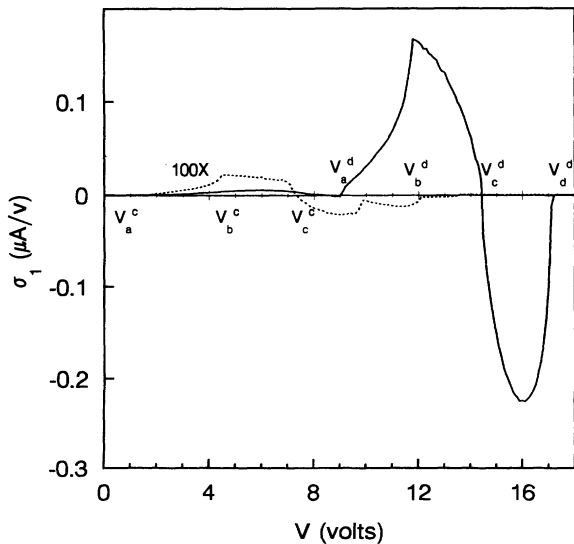


FIG. 4. Conductance vs voltage curves. The solid line is the discrete case and the dashed line is the continuum case.

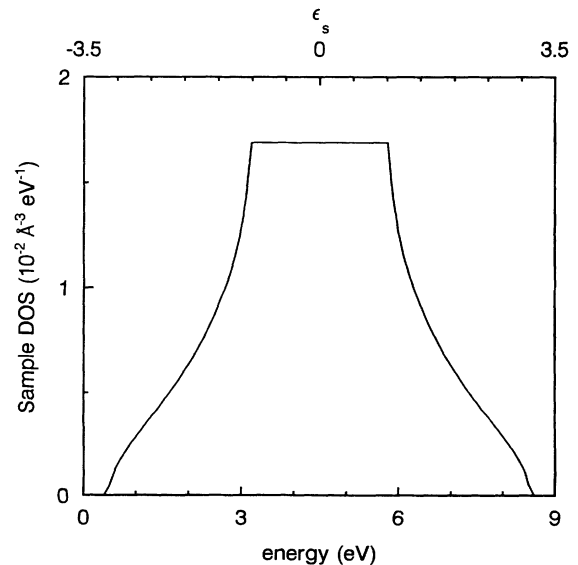


FIG. 5. Sample DOS. The horizontal axis is labeled in eV and adimensional units corresponding to  $\epsilon_s$ .

Eq. (21) is in the small region around the points for which  $\sin\theta_3=0$ , and therefore this equation simplifies to

$$\sigma_1 = \frac{2\pi e^2 A^2}{\hbar} \frac{1}{(2\beta_s)^2} c_k^2 [\Theta(E_F - E_k^{\text{Tip}}) - \Theta(E_F - E_k^{\text{Tip}} - V)] \times \frac{1}{1+z^2} \left| \sum_{m_1, m_2} (-1)^{m_1} (-1)^{m_2} e^{-(\sqrt{d^2 + \rho_m^2})/a_s} \right|^2, \quad (22)$$

where the sum reduced to the term  $k$  corresponding to the discrete state, at which the electron has about 90% probability of being. The integral in Eq. (21) is proportional to the surface integral in  $\theta$  space of the inverse of the gradient of the energy, that is, the global density of states DOS.

$$\sigma_1(V \approx V_a) \propto \text{DOS}(\epsilon_s \approx -3). \quad (23)$$

Following a similar reasoning for voltages close to  $V_b$ ,

$$\sigma_1(V \approx V_b) = C_1 + C_2 \text{DOS}(\epsilon_s \approx -1), \quad (24)$$

where  $C_1$  and  $C_2$  are constants.<sup>37</sup>

A smooth, monotonically increasing function  $\sigma_1(V)$  that has an infinite slope at  $V_a$  and  $V_b$  and satisfies Eqs. (23) and (24) must closely follow the shape of  $\text{DOS}(\epsilon_s)$  for  $-3 \leq \epsilon_s \leq -1$ . For voltages between  $V_b$  and  $V_c$ , corresponding to  $-1 < \epsilon_s < 1$ , there are no critical points in the region of integration and the integrals of  $\cotan(\theta_3)$  and  $1/\sin(\theta_3)$  are different. At  $V_c$ , we can see that the slope of the conductance is infinite, corresponding to another Van Hove singularity. Since  $\sigma_1(V_c)=0$ , the shape of  $\sigma_1(V)$  for  $V_c < V < V_d$  cannot and does not follow the corresponding DOS shape.

Let us next analyze the continuous case. Immediately one can see that for the region of voltages with negative conductances, there does not exist any straightforward shape relationship between the conductance and DOS.

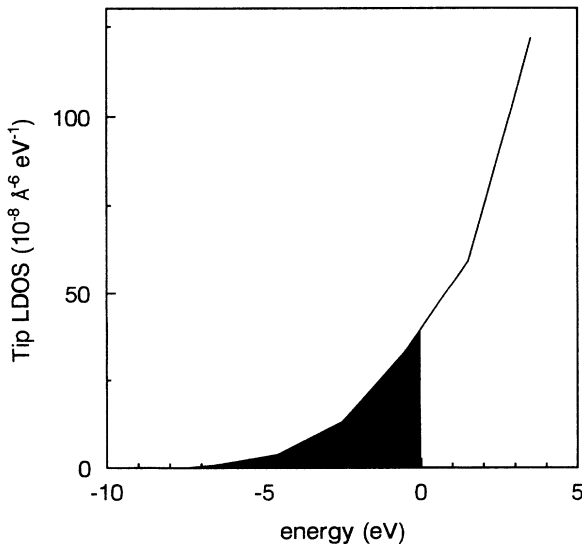


FIG. 6. Tip LDOS. The dark region corresponds to the occupied states below the Fermi energy.

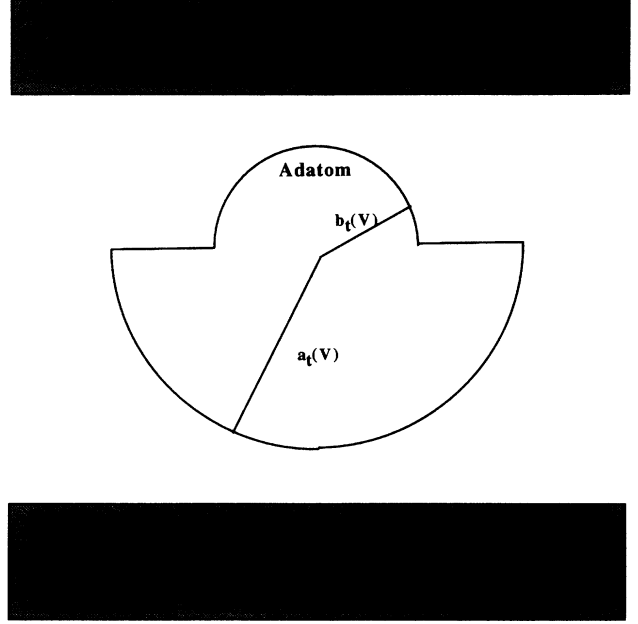


FIG. 7. Distortion of the tip adatom wave function as a result of an applied electric field.

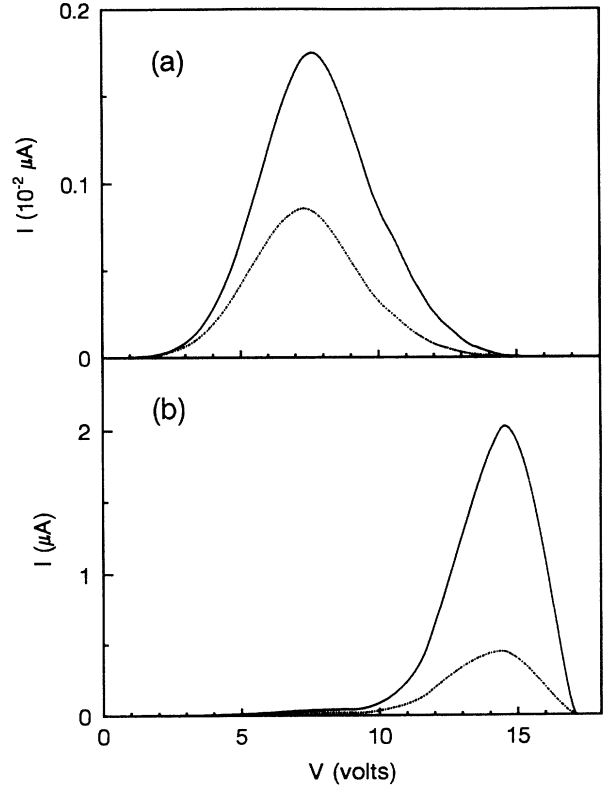


FIG. 8. Current vs voltage. The dotted-dashed lines correspond to the results in Fig. 2(a). The solid lines correspond to the results calculated with the wave function from Fig. 7. (a) Continuum case. (b) Discrete case.

For  $V_a \leq V \leq V_c$ , the shape of  $\sigma_1(V)$  seems to follow DOS ( $-3 \leq \epsilon_s \leq 1$ ). For  $V_a \leq V \leq V_b$ , an argument similar to the discrete case holds, in which now the role played by the discrete state is taken by levels close to the Fermi energy of the tip, since they are the ones that have the largest LDOS (see Fig. 6). For  $V_b < V \leq V_c$  we see a slowly decreasing  $\sigma_1(V)$ . This is roughly the product of the

maximum of the sample DOS (taken at  $\epsilon_s = -1$ ) times the LDOS of the tip for the tip state whose energy is aligned with  $\epsilon_s = -1$ . The slow decreasing behavior of  $\sigma_1$  in this region is then an effect of the decrease of the tip LDOS with decreasing energies. So in this region,  $\sigma_1(V)$  is a map of the tip states and not the sample states. The second term in  $dI/dV$  is

$$\sigma_2 = \frac{2\pi e^2 A^2}{\hbar} \sum_k c_k^2 \delta(E_F - E_k^{\text{Tip}} - V) \int d\theta_1 d\theta_2 \frac{\sin^2(N\theta_3)}{\sin\theta_3} \left| \sum_{n_1, n_2} e^{i(n_1\theta_1 + n_2\theta_2)} e^{-(\sqrt{d^2 + \rho_n^2})/a_s} \right|^2. \quad (25)$$

Due to the presence of the  $\delta$  function, the sum in  $k$  is restricted to those values for which  $E_k = E_F - V$ . The integral in Eq. (25) at those energies is the sample LDOS evaluated at  $\epsilon_s$  corresponding to  $E_s = E_F$ . Then  $\sigma_2(V)$  vanishes because there are no sample states in the band gap.

### III. EFFECT OF THE FINITE BARRIER SIZE

The results of the previous section provide a background relevant to interpret STS experimental data. However we did not take into consideration the deformation of the wave function in the vacuum due to the sample-tip electric field. The reason for this is that the barrier was implicitly considered to be very tall, so that variations in the voltage change the energy levels but do not change the spatial shape of the wave functions. For semiconductors the work function is a few eV, the same order of magnitude of the tip-sample voltages (times  $e$ ) used in STS. Therefore, in practice the change of the shape of the wave functions has to be considered. One knows that the smaller the effective barrier, the more the electron adatom wave function will elongate towards the sample. In order to gauge the effect of this elongation we work out the following simple model.

We consider the situation as in Fig. 7. There, it is shown in a simple way how one can make the wave function decay less in the barrier region than in the tip-bulk region. A simple calculation in the context of a hydrogenic atom shows that the "decay length" as a function of applied voltage,  $a_t(V)$ , is given in terms of  $a_t$ , the zero-voltage decay length, as

$$a_t(V) = \frac{a_t}{\left[ 1 - \frac{2 \text{ meV } a_t^2}{\hbar^2} \right]^{1/2}}. \quad (26)$$

In Fig. 8 we show a comparison of the  $I$ - $V$  curves between the "zero-voltage wave function" case and the case in which Eq. (26) was used. We observe that the effect of the electric field in the wave function produces an in-

crease in the current. This is due to the enhancement of the tunneling probability as the effective barrier height decreases with increasing voltage. Since within our simple assumption for  $a_t(V)$  both currents are of the same order of magnitude and have similar shapes, the arguments presented in the previous sections hold true.

### IV. CONCLUSIONS

We have introduced a model that serves to understand the relationship between  $I$ - $V$  curves and densities of states for semiconductor samples. This was done within the intrinsic constraints dictated by an  $s$ -wave band tight-binding approach, and Bardeen's theory of tunneling. The tip was considered to be a system of an atom adsorbed on a solid surface. A feature of our results is the introduction of results for a tip configuration in which a discrete state exists below the continuum of the conduction-band states.

We found that the  $I$ - $V$  curve in the discrete case resembles the sample LDOS. In the continuous case, the  $I$ - $V$  curve is a convolution of tip and sample LDOS. On the other hand,  $dI(V)/dV$  follows the sample DOS for voltages that scan sample states from the bottom of the band to the first Van Hove singularity. From there to the next singularity,  $dI(V)/dV$  for the continuous case follows the shape of the tip LDOS.

Finally, we presented a simple way in which the adatom wave-function barrier penetration affects the  $I$ - $V$  curves and we found that although it produces an increase in the current, the effect is not large enough to change our understanding of the underlying physics explained above.

### ACKNOWLEDGMENTS

We thank Professor Abraham Many for helpful insights. This work was supported by NASA-JOVE, NSF-RCSE (F.R.Z.), and NSF EHR-9108775 (L.F.F. and Y.G.).

<sup>1</sup>R. M. Feenstra, J. Vac. Sci. Technol. B 7, 925 (1989).

<sup>2</sup>P. Avouris and I. Lyo, Surf. Sci. 242, 1 (1991).

<sup>3</sup>R. J. Hamers, R. M. Tromp, and J. E. Demuth, Phys. Rev. Lett. 56, 1972 (1986).

<sup>4</sup>H. F. Hess, R. B. Robinson, R. C. Dynes, J. M. Valles, Jr., and

J. V. Waszczak, J. Vac. Sci. Technol. A 8, 450 (1990).

<sup>5</sup>L. C. Davis, M. P. Everson, R. C. Jaklevic, and W. Shen, Phys. Rev. B 43, 3821 (1991).

<sup>6</sup>J. Tersoff and D. R. Hamann, Phys. Rev. B 31, 805 (1985).

<sup>7</sup>N. D. Lang, Phys. Rev. Lett. 55, 230 (1985).

- <sup>8</sup>N. D. Lang, Phys. Rev. Lett. **55**, 2925 (1985).  
<sup>9</sup>C. J. Chen, J. Vac. Sci. Technol. A **6**, 319 (1988).  
<sup>10</sup>C. R. Leavens and G. C. Aers, Phys. Rev. B **38**, 7357 (1988).  
<sup>11</sup>E. Tekman and S. Ciraci, Phys. Rev. B **40**, 10 286 (1989).  
<sup>12</sup>S. Ciraci and E. Tekman, Phys. Rev. B **40**, 11 969 (1989).  
<sup>13</sup>C. J. Chen, Phys. Rev. Lett. **65**, 448 (1990).  
<sup>14</sup>G. Doyen, D. Drakova, and M. Scheffler, Phys. Rev. B **47**, 9778 (1993).  
<sup>15</sup>N. D. Lang, Phys. Rev. B **34**, 5947 (1986).  
<sup>16</sup>A. Selloni, P. Carnevalli, E. Tosati, and C. D. Chen, Phys. Rev. B **31**, 2602 (1985).  
<sup>17</sup>M. Tsukada, K. Kobayashi, N. Isshiki, and H. Kageshima, Surf. Sci. Rep. **13**, 2 (1991).  
<sup>18</sup>R. Tromp, J. Phys. Condens. Matter **1**, 10 211 (1989).  
<sup>19</sup>R. J. Hamers, in *Scanning Tunneling Microscopy I*, edited by H. J. Güntherodt and R. Wiesendanger, Springer Series in Surface Sciences Vol. 20 (Springer-Verlag, Berlin, 1992).  
<sup>20</sup>R. J. Hamers, Annu. Rev. Phys. Chem. **40**, 531 (1989).  
<sup>21</sup>J. Bardeen, Phys. Rev. Lett. **6**, 57 (1961).  
<sup>22</sup>A. A. Lucas, Europhys. News **21**, 63 (1990).  
<sup>23</sup>N. F. Mott and H. Jones, *The Theory of the Properties of Metals and Alloys* (Dover, New York, 1958).  
<sup>24</sup>T. L. Einstein, Surf. Sci. **45**, 713 (1974).  
<sup>25</sup>T. L. Einstein, Phys. Rev. B **12**, 1262 (1975).  
<sup>26</sup>T. L. Einstein and J. R. Schrieffer, Phys. Rev. B **7**, 3629 (1973).  
<sup>27</sup>D. Kalkstein and P. Soven, Surf. Sci. **26**, 85 (1971).  
<sup>28</sup>T. B. Grimley, J. Phys. Chem. Solids **14**, 227 (1960).  
<sup>29</sup>M. Posternak, H. Krakauer, A. J. Freeman, and D. D. Koelling, Phys. Rev. B **21**, 5601 (1980).  
<sup>30</sup>J. A. Applebaum and D. R. Hamann, Phys. Rev. Lett. **31**, 106 (1973).  
<sup>31</sup>C. J. Chen, Phys. Rev. B **42**, 8841 (1990).  
<sup>32</sup>R. H. Fowler and L. Nordheim, Proc. R. Soc. London, Ser. A **119**, 173 (1928).  
<sup>33</sup>R. S. Becker, J. A. Golovchenko, D. R. Hamann, and B. S. Swartzentruber, Phys. Rev. Lett. **55**, 2032 (1985).  
<sup>34</sup>J. Ferrer, A. Martin-Rodero, and F. Flores, Phys. Rev. B **38**, 10 113 (1988).  
<sup>35</sup>W. Sacks and C. Nogra, Phys. Rev. B **43**, 11 612 (1991).  
<sup>36</sup>R. M. Feenstra, J. A. Stroscio, and A. P. Fein, Surf. Sci. **181**, 295 (1987).  
<sup>37</sup>J. M. Ziman, *Principles of the Theory of Solids*, 2nd ed. (Cambridge University Press, England, 1972), Sec. 2.5.



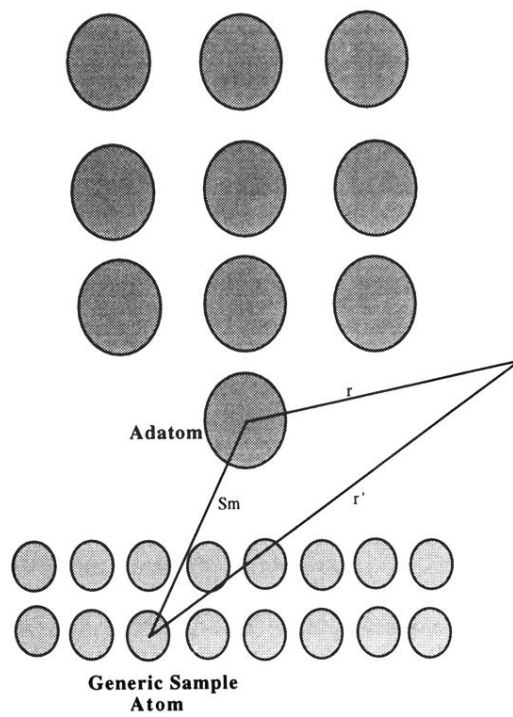


FIG. 1. Sagittal cross section of the atomic arrangement for the tight-binding and  $M_{TS}$  calculations.

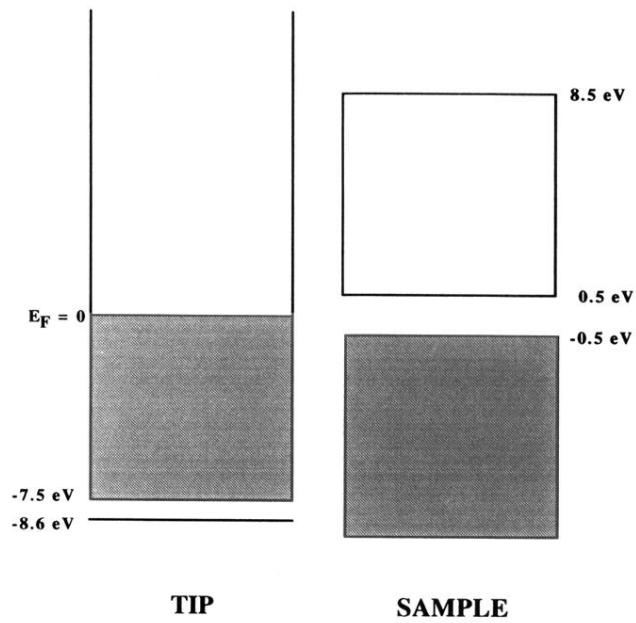


FIG. 3. Energy-level diagrams for the tip and the sample for zero applied voltage for the discrete case. The voltage convention is such that as the bias voltage increases, the tip energy levels more upwards with respect to the sample energy levels. The dark regions represent occupied states. The horizontal line at the bottom of the tip diagram corresponds to the discrete level. The continuum case energy diagram is obtained from this one by just removing the discrete state.

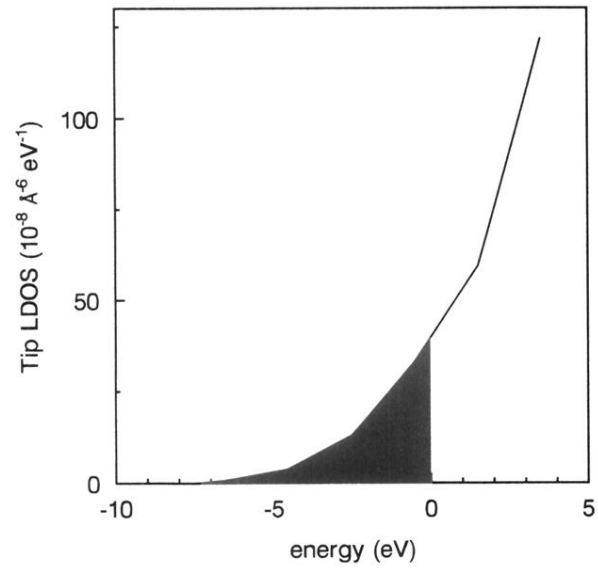


FIG. 6. Tip LDOS. The dark region corresponds to the occupied states below the Fermi energy.

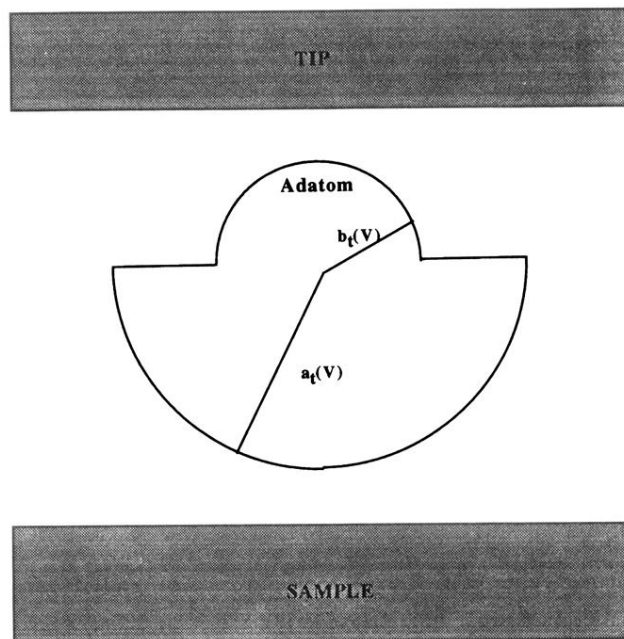


FIG. 7. Distortion of the tip adatom wave function as a result of an applied electric field.